Supporting online material for

Reversal of RNA-dominance by displacement of protein sequestered on triplet repeat RNA

Thurman M. Wheeler, Krzysztof Sobczak, John D. Lueck, Robert J. Osborne, Xiaoyan Lin, Robert T. Dirksen, Charles A. Thornton

This pdf includes:

Materials and Methods

Morpholino oligonucleotides. Morpholino oligonucleotides were purchased from Gene Tools (Philomath, OR). The sequence of CAG25 was: 5′-AGCAGCAGCAGCAGCAGCAGCAGCA-3′. The control morpholino of unrelated sequence was: 5′- GAAGAGACAACGTCTGGCACGGACC-3′. The GAC25 inverted control was: 5′-ACGACGACGACGACGACGACGACGA-3′.

Preparation of CUG^{exp} RNA and recombinant MBNL1 protein. $(CUG)_{109}$ transcripts were enzymatically synthesized using T7 RNA polymerase and plasmid pCUG^{exp}-tail as template. The plasmid was linearized by digestion with BamHI (for RNA containing only CUG repeats) or XbaI (for CUG repeats with a 3′-anchoring tail). Transcription was carried out in 50 μl containing 2 μg of digested pCUG^{exp}-tail plasmid, 3.5 mM rNTPs, 3.5 mM guanosine, 4 μl of enzymatic mixture (T7 RNA polymerase and RNase inhibitors) from MegaScript-T7 kit (Ambion) and 1x reaction buffer from the same kit. Transcripts were purified on denaturing 6% polyacrylamide gels. Similar methods were used to synthesize $(CUG)_{54}$ RNA. For mapping of CAG25 binding sites, the CUG^{exp} RNA was 5′-end-labeled with T4 polynucleotide kinase and [γ^{32}P]ATP (4500 Ci/mmol; ICN). The labeled RNA was re-purified by electrophoresis on denaturing polyacrylamide gels. Fluorescently-labeled RNA (Fl-CUG^{exp}) was internally labeled by *in vitro* transcription using 0.15 mM fluorescein-UTP (Roche) and unlabeled 0.5 mM ATP, 0.5 mM CTP, 0.5 mM GTP, and 0.35 mM UTP (percentage of incorporated labeled U-residues was about 10%). Recombinant full length MBNL1 protein was prepared as previously described using BL21(DE3) cells and pGEX-6P-MBNL1-His vector (*1*). Purified protein (5 μM) was stored at –70°C in solution containing 50 mM Tris-HCl (pH 8.0), 50 mM NaCl, 50 mM KCl and 50% glycerol.

Chemical and enzymatic mapping of CAG25 morpholino binding to CUG^{exp} RNA. A 5′-end ^{32}P-labeled $(CUG)_{54}$ transcript was purified on denaturing gels. The transcript was denatured by heating at 80°C for 1 min in 50 mM Tris–HCl (pH 8.0), 50 mM KCl, 50 mM NaCl and 1 mM $MgCl_2$ (buffer A) supplemented with 0.5 mM DTT, following by renaturation at RT. The end-labeled transcript (2 nM) was incubated with the indicated concentration of CAG25 in buffer A at 37°C for 30 min. Limited RNA digestion was initiated by mixing 5 μl of RNA only (control) or RNA/morpholino sample with 5 μl of a probe solution containing either lead ions or ribonuclease T1 in reaction buffer. The RNA hydrolysis was performed at 37°C for 15 min and terminated by adding an equal volume of stop solution (7.5 M urea and 20 mM EDTA with dyes) and sample freezing. To determine the cleavage sites, the products of RNA fragmentation were separated on preheated 10% polyacrylamide gels containing 7.5 M urea, 14 M formamide, 90 mM Tris-borate buffer and 2 mM EDTA, along with the products of alkaline hydrolysis and limited T1 nuclease digestion of the same RNA. The alkaline hydrolysis ladder was generated by the incubation of the labeled RNA in formamide containing 0.5 mM $MgCl_2$ at 100°C for 10 min. The partial T1 ribonuclease digestion of RNA was performed under semi-denaturing conditions (10 mM sodium citrate, pH 5.0; 3.5 M urea) with 0.2 U/μl of the enzyme during incubation at 55°C for 10 min. Electrophoresis was performed at 1800 V (gel dimensions, 30/50 cm). The products of the structure probing reactions were visualized by phosphorimaging and quantified with ImageQuant (Molecular Dynamics).

Electrophoretic mobility shift assay (EMSA) for CUG^{exp}-CAG25 binding and formation of CUG^{exp}-MBNL1 complex. Gel-purified fluorescently-labeled $(CUG)_{109}$ RNA was denatured and renatured as described above. To analyze $(CUG)_{109}$/CAG25 binding, $(CUG)_{109}$ (2 nM final

concentration) was incubated with the indicated concentration of CAG25 in buffer A (also containing 50 μg/ml acetylated BSA and 5% glycerol) for 30 min at 37°C. To analyze the effects of CAG25 on CUG^{exp}-MBNL1 binding, recombinant MBNL1 (250 nM) was incubated with $(CUG)_{109}$ (5 nM) for 30 min at 37°C. Because MBNL1 binds as few as 6 bp of CUG repeat duplex (*2*), and MBNL1 binding capacity of CUG^{exp} increases in proportion to length of the CUG repeat (*1, 3*), the $(CUG)_{109}$ transcripts can interact with one to many copies of MBNL1, resulting in a gel shift that appears as a heterogeneous smear rather than a discreet band. The indicated concentration of CAG25 was added to $(CUG)_{109}$ RNA before (to inhibit formation of RNA-protein complex; "prevention") or after (to disrupt pre-formed RNA-protein complex; "displacement") addition of MBNL1 protein. Samples were immediately loaded onto 1.5% agarose gels buffered with 1x Tris-borate and electrophoretically separated at 100 V for 1-2 h. Gels were scanned on a laser fluorescence imager (Molecular Dynamics) and analyzed by ImageQuant 5.2 (Molecular Dynamics).

Microtiter plate assay for prevention or disruption of CUG^{exp}-MBNL1 binding. 25 pmoles of 5′-biotinylated "capture" oligodeoxynucleotide (5′-TTTTAATTTTAGGATCCCCCCAG-3′) was bound to each well of a 96-well streptavidin-coated microtiter plate (Reacti-Bind Streptavidin Coated Plates-HBC; Pierce) by incubation in 1x TE buffer for 2 hrs at RT, followed by aspiration and washing with buffer A. CUG^{exp}-tail transcript (5 pmoles in buffer A), which has $(CUG)_{109}$ followed by 3′-sequence complementary to the "capture" oligo, was added to plates, incubated 45 min, and washed once, resulting in 0.2-0.4 pmol of $(CUG)_{109}$ transcript tethered in each well. To analyze prevention of CUG^{exp}-MBNL1 complex formation, plates loaded with CUG^{exp}-tail transcript were incubated for 30 min with the indicated concentration of CAG25 in buffer A supplemented with 0.05% Tween. Recombinant MBNL1 protein was then added to a final concentration 250 nM (50- to 100-fold molar

excess of protein to RNA), and samples were incubated for 30 min at 37°C. To analyze disruption of preformed CUG^{exp}-MBNL1 complexes, the order of addition for CAG25 and MBNL1 protein was switched. Following either procedure, unbound protein was aspirated and wells were washed with buffer A containing 0.05% Tween. To elute and quantify MBNL1 retained in wells, RNA was cleaved by RNase H/RNase A (10 min) followed by addition of 2x SDS-gel loading buffer (100 mM Tris-Cl (pH 6.8), 4% SDS, 200 mM β-mercaptoethanol and dyes). Samples were denatured and analyzed on 10% SDS-polyacrylamide gels. Gels were stained overnight in SyproRuby (Invitrogen) according to manufacturer recommendations. Protein was visualized using a laser fluorimager (Molecular Dynamics) and quantified using ImageQuant. Inhibition curves were obtained using GraphPad Prism software. The % MBNL1 bound that remained bound to CUG^{exp} was expressed as the mean ± SD of protein retained on plate, normalized for 100% retention in the absence of CAG25, $n = 4$ independent experiments. IC50 values similar to those reported in Fig. 1 were also obtained at a lower MBNL1 concentration of 100 nM.

Filter binding assay for CAG25 binding to CUG^{exp} RNA. 5′-end ^{32}P-labeled $(CUG)_{109}$ was gel-purified, denatured, and renatured as described above, and then incubated for 30 min at 37°C in buffer A (final concentration 0.5 nM) with the indicated concentration of CAG25. Samples were then applied to a slot manifold containing pre-wetted membranes [order from top: nitrocellulose membrane (BioRad), Hybond-N+ nylon membrane (Amersham Pharmacia Biotech) and Whatman 3 mm blotting paper], followed by a single wash with buffer A. The membranes were air-dried and exposed to a phosphorimager screen and signal quantified using ImageQuant software. Due to the non-ionic character of the morpholino backbone, we determined in pilot experiments that >95% of CAG25 was captured on the nitrocellulose membrane. CAG25 binding caused retention of $(CUG)_{109}$ on

nitrocellulose, whereas unbound $(CUG)_{109}$ passed through the nitrocellulose and was captured on the nylon.

Transgenic and knockout mice. Animal experiments were approved by the University Committee on Animal Resources at the University of Rochester Medical Center. All mice used in these studies were on the FVB inbred background. Homozygous human skeletal actin long repeat (HSA^{LR}) transgenic mice in line 20b, human skeletal actin short repeat (HSA^{SR}) transgenic mice, and *Mbnl1* knockout mice were previously described (*4*, *5*).

Muscle injection of morpholinos. Tibialis anterior (TA) or flexor digitorum brevis (FDB) muscles were injected with 20 μg of CAG25 or control morpholino in 20 μl of PBS, or with PBS alone, followed by electroporation as described previously (*6*). For all TA muscles to be analyzed by electromyography (EMG), treatment assignment of CAG25 vs. vehicle (right vs. left side) were randomized and EMG analysis was performed by an examiner who was blinded to the treatment assignment.

Cell culture. Human DM1 fibroblasts from cell lines GM03132 were purchased (Coriell Institute, Camden, NJ) and maintained in Eagle's minimum essential medium, 15% fetal bovine serum, 1% penicillin/streptomycin, and 5% CO_2 at 37°C. Cells were transfected with CAG25 morpholino (40 μM) together with the transfection reagent EndoPorter (Gene Tools) or EndoPorter alone, according to manufacturer instructions. Cells were analyzed 48 hours after transfection.

Fluorescence *in situ* hybridization (FISH). Individual FDB muscle fibers were isolated as described previously (*7*). For FISH with human-specific skeletal actin (HSA) probe, FDB fibers were plated on glass coverslips, fixed in 3% PFA for 15 minutes at room temperature (RT), washed in PBS, and permeabilized in 0.5% Triton X-100/PBS for 5 minutes at RT. Hybridization was carried out as previously described (*8*), except formamide concentration was 25% throughout, hybridization time was 3 hours, and post-hybridization wash was at RT. The HSA probe was DNA oligonucleotide 5′-CTGTGTCAGTTTACGATGGCAGCAAC-3′, 5′-end-labeled with Cy5 (IDT). FDB fibers also were hybridized with a CAG-repeat 2′-O-methyl oligoribonucleotide probe 5′-labeled with Texas Red as described previously (*8*), except that permeabilization was achieved by 0.5% Triton-X 100 (Sigma) in PBS for 5 minutes at RT instead of 2% acetone/PBS. Untreated, vehicle-treated, and CAG25 morpholino-treated human DM1 cells were hybridized with the same CAG-repeat 2′-O-methyl oligoribonucleotide probe.

Immunofluorescence. FDB fibers were fixed in 2% PFA/PBS (pH 7.3) for 5 minutes at RT, washed in PBS/0.05% Tween-20, permeabilized in pre-chilled 50% methanol/50% acetone for 10 minutes at –20º C, washed in PBS/0.05% Tween-20, blocked in 5% normal goat serum, and placed in primary antibody (anti-MBNL1 A2764 1:2000 in 1% BSA/PBS) overnight at 4º C. Fibers then were washed in 1% BSA/PBS, placed in secondary antibody (goat anti-rabbit Alexa 488 1:400 in 1% BSA/PBS) with nuclear counterstain (4,6 diamino-2-phenylindole dihydrochloride; DAPI, 1:20,000 in PBS) 1 hour RT, washed in 1% BSA/PBS followed by a final wash in PBS, mounted on glass slides, and sealed with fingernail polish. Specificity of this antibody was previously shown (*8*). Control experiments included treatment of a parallel set of fibers without primary antibody. FISH/IF on cryosections of TA muscles

three weeks after injection with CAG25 morpholino or saline was performed as described previously (*8*). ClC-1 protein was detected on transverse sections of TA muscles as described previously (*6*).

RT-PCR analysis of alternative splicing. Total RNA was isolated from TA muscles 3 and 14 weeks after injection with CAG25, control morpholino, or saline. cDNA synthesis and alternative splicing analyses for ClC-1, Serca-1, m-Titin and Zasp were performed as described previously (*6*, *8*).

Macroscopic recordings of ClC-1 currents. Delivery of control and CAG morpholinos into FDB fibers was achieved by injection and electroporation of hindlimb footpads as described previously (*6*). Three to five days after injection and electroporation, individual FDB muscle fibers were isolated and whole cell ClC-1 currents recorded using approaches identical to those described in detail elsewhere (*7*).

Electromyography. EMG analysis of myotonia was performed under general anesthesia by a blinded examiner as described previously (*6*). Myotonia was graded as follows: 0 indicates no myotonia; 1, occasional myotonic discharge in less than 50% of electrode insertions; 2, myotonic discharge in greater than 50% of insertions; 3, myotonic discharge with nearly every insertion. WT mice do not show myotonia by these methods.

Analysis of CUG^{exp} in cytoplasm-enriched fractions. Four weeks after injection with saline or CAG25 morpholino, freshly isolated TA muscle was minced with scissors in 1 ml lysis buffer (20 mM Hepes, pH 7.5, 10 mM KCl, 1 mM EDTA, 2mM $MgCl_2$), briefly homogenized, and centrifuged at 2000 x *g* for 10 minutes. The supernatant from this initial spin contains the cytoplasm-enriched

fraction. To isolate RNA from the cytoplasm-enriched fraction, the supernatant, was transferred to a new tube and centrifuged at 10,000 x *g* for 10 minutes. Cytoplasmic RNA was extracted from the supernatant using TRI Reagent LS (Molecular Research Center, Cincinnati, OH). Linear acrylamide was added during RNA precipitation. For comparison of human- relative to mouse-skeletal actin, the skeletal actin cDNA from both species was amplified by the same primer set: HSA16 (forward, 5′-GACATCGACATCAGGAAGGACC-3′) and HSA17 (reverse, 5′-CCTCGTCGTACTCCTGCTTGG-3′) (30 cycles). These primers are perfectly complementary to cDNA from both species. The PCR products were purified, digested with restriction enzyme AluI (cuts actin cDNA from mouse but not human), separated on agarose gels, stained with SYBR Green (Invitrogen), and imaged on a laser scanner. The depletion of nuclear RNA from cytoplasmic fractions was determined by RT-PCR for the 5′ external transcribed spacer (5′ ETS) of ribosomal RNA. The 5′ ETS is cleaved prior to export of rRNA from the nucleus. The primer set was mrRNAETS-f-B (forward, 5′-GTGACTTTGCTGCGTGTCAGAC-3′) AND mrRNAETS-r-B (reverse, 5′-CCACAGACAGGAGTGAAGTACTCG-3′). The cycle number was 20.

Derivation of LLC9 mice with conditional expression of CUG^{exp} RNA and *in vivo* imaging for luciferase activity. The LLC9 transgene diagrammed in Fig. 4B was constructed by standard cloning methods using the following fragments: CMV enhancer fused to chicken beta actin promoter (J. Miyazaki, Osaka, Japan), “triple stop” transcriptional terminator element (TTE) from C. Lobe (Toronto, Ontario), chicken beta globin insulators (G. Felsenfeld, Bethesda, MD), firefly luciferase, and human DMPK 3′ UTR cloned from muscle cDNA. LLC9 transgenic mice were derived by conventional transgenesis on the FVB inbred background, and maintained on this background. To excise the TTE and permit transcription of the $(CTG)_{270}$ repeat, LLC9 mice were bred to Rosa-CreER

transgenic mice that express tamoxifen-inducible *cre* recombinase. The terminator element was excised, and expression of luciferase mRNA containing $(CUG)_{270}$ in the 3′ UTR (CUG^{exp}) was induced, by daily intraperitoneal injection of bitransgenic mice with 1 mg tamoxifen (10 mg/ml in 90% canola oil/10% ethanol) for a total of 8 doses. One week after induction, the mice were injected with 20 μg CAG25 morpholino in one TA and saline in the contralateral TA. Luciferase activity was quantitated 2-7 weeks later using an *in vivo* imaging system (IVIS; Xenogen, Alameda, CA) and software (Living Image, Xenogen) as described previously (*9*).

Northern and slot blot analysis of CUG^{exp} transcripts. For Northern analysis, 3 or 6 μg of the total RNA was separated on 1.2% agarose-MOPS gels containing 1.5% formaldehyde for 1.5 h at 80V. Alkaline fragmented RNA was transferred onto Hybond-N+ membrane (Amersham Pharmacia Biotech) by capillary transfer with 10x SSC. Blots were hybridized with 5′-end ^{32}P-labeled oligonucleotide probes specific either for human skeletal actin transgene (5′-CTGTGTCAGTTTACGATGGCAGCAAC-3′) or endogenous mouse skeletal actin (5′-ACCCTGCAACCACAGCACGATTGTCGATTG-3′, loading control) in a buffer containing 250 mM Na_2HPO_4 pH 7.5, 7% SDS, 1 mM EDTA and 1% BSA at 42°C overnight, or for 3 hours at 37° in ExpressHyb solution (Clontech) according to manufacturer recommendations. Blots were washed twice with 2X SSC and 0.5% SDS, once with 0.5X SSC and 0.5% SDS, analyzed on a phoshorimager, and quantified using ImageQuant. Hybridization conditions for slot-blot analysis of CUG^{exp} RNA were the same, except that end-labeled $(CAG)_8$ was used as probe.

CAG25-dependent degradation of $(CUG)_{109}$ by RNase H or HeLa cell extracts. Fluorescently-labeled $(CUG)_{109}$ RNA was denaturated and renatured as described above. $(CUG)_{109}$ RNA (2.5 nM)

was incubated with 2.5 μM CAG25 morpholino or CAG25-DNA in buffer A at 37°C for 30 min. Under these conditions both oligomers form a heteroduplex with $(CUG)_{109}$ RNA. The indicated amount of recombinant RNase H (Invitrogen) was added and incubated for an additional 30 min. Reactions were stopped by adding an equal volume of gel loading buffer (8 M urea, and 20mM EDTA with dyes). Samples were separated on 10% polyacrylamide/7.5 M urea/14 M formamide gels run in 1x TBE buffer. Fluorescence was visualized directly on a laser fluorimager (Molecular Dynamics). Whole cell extract was prepared from 6 x 10^7 HeLa cells growing in log phase. The cells were pelleted and washed twice in phosphate-buffered saline and resuspended in a double volume of hypotonic swelling buffer (7 mM Tris-HCl, pH 7.5, 7 mM KCl, 1 mM $MgCl_2$, 1 mM β-mercaptoethanol) and after 10 min incubation on ice, they were homogenized 20-times in Dounce homogenizer followed by the addition of one-tenth of the final volume of the neutralizing buffer (21 mM Tris-HCl, pH 7.5, 116 mM KCl, 3.6 mM $MgCl_2$, 6 mM β-mercaptoethanol). Finally, homogenates were centrifuged at 21,000 x *g* for 5 min at 4°C, and supernatants were stored at –70 °C with 40% glycerol. Degradation of radio-labeled $(CUG)_{109}$ (250 pM) complexed with different oligomers was performed as described above using one-tenth volume of whole HeLa cell extract instead of recombinant RNase H and incubated at RT for the indicated period of time.

Statistics. Group data are expressed as mean ± SD, except for patch clamp data in Fig 3 and Fig S7, which are expressed as mean ± SEM. Between group comparison was performed by two-tailed Student's *t* test or two-way ANOVA, as indicated. A *P* value of < 0.05 was considered significant.

Supporting Figures

Fig. S1

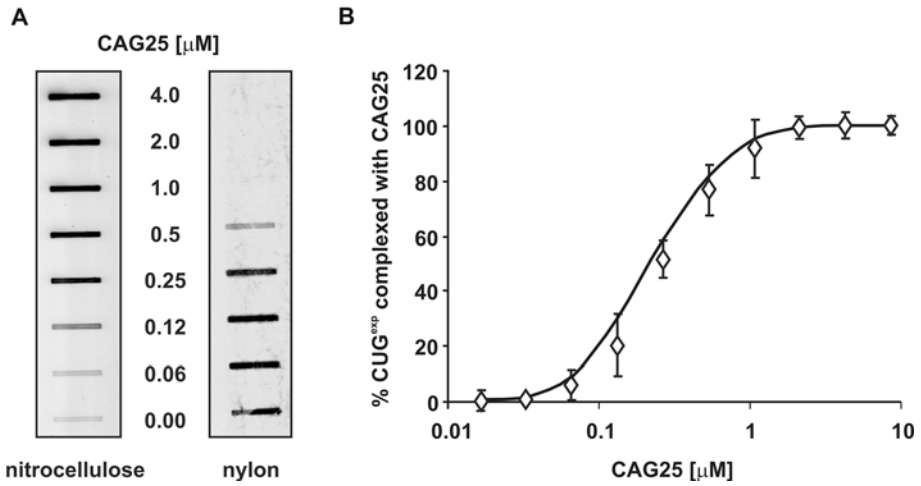

Fig. S1. (A) Filter binding assay for CAG25 hybridization to CUG^{exp} RNA. ^{32}P end-labeled $(CUG)_{109}$ (0.5 nM) was incubated with the indicated concentrations of CAG25 for 30 min at 37°C, then applied to a slot manifold [nitrocellulose membrane on top, nylon membrane in the middle, blotting paper on the bottom] followed by a single wash. $(CUG)_{109}$/CAG25 heteroduplex is retained on the top layer (nitrocellulose), whereas unbound $(CUG)_{109}$ passes through and is retained on the nylon membrane. Approximately half the $(CUG)_{109}$ transcript is complexed with morpholino at a concentration of 250 nM CAG25 (similar signal at both filters). **(B)** Quantitation of the results shown in A. Data are the mean ± SD from three independent experiments. The apparent dissociation constants were calculated using a one-site binding model and GraphPad Prism software. The estimated Kd for $(CUG)_{109}$/CAG25 binding was 232 ± 47 nM, though this may underestimate morpholino binding that occurs in cells through protein-facilitated hybridization.

Fig. S2

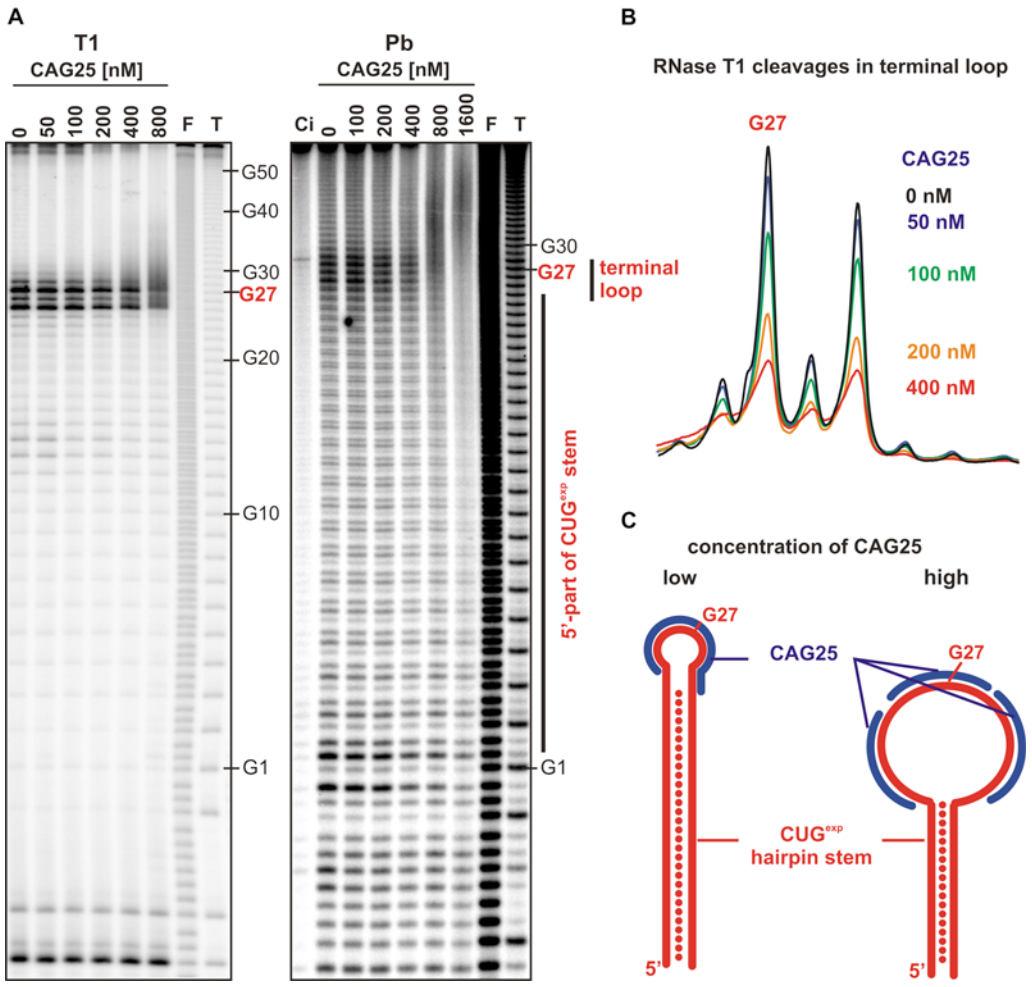

Fig. S2. *In vitro* mapping of CAG25 binding shows that initial invasion of CUG^{exp} hairpin occurred by binding within the terminal loop, thus opening the loop and increasing the access to hybridization along the stem. **(A)** Autoradiogram showing that CAG25 binds initially within the terminal loop region of $(CUG)_{54}$ RNA. Binding sites for CAG25 were mapped using two structure-dependent probes: 0.5 mM lead (Pb) ions, or 1.5 units/µl RNase T1 (T1). Prior to the addition of probe, the 5′-end ^{32}P-labeled $(CUG)_{54}$ transcript (2 nM) was incubated with the indicated concentration of CAG25 for 30 min at 37°C. Pb ions cleave single-stranded RNA regions and, to a lesser extent, relaxed

portions of duplex RNA. RNase T1 cleaves single-stranded RNA after guanosine nucleotides. In the absence of CAG25 morpholino (lane "0"), cleavage occurs predominantly in the terminal loop of the $(CUG)_{54}$ hairpin, at guanosine 27 ("G27", midpoint of the repeat tract, where "G1" marks the 5′-most CUG repeat). CAG25 suppresses cleavage by both probes, with initial protection preferentially in the terminal loop, and, at higher concentration of CAG25, subsequent protection within the stem (more evident with Pb cleavage). Lane Ci, no probe added; lane F, statistical cleavage by Mg^{++} under denaturing conditions; lane T, guanosine-specific ladder obtained by cleavage with T1 ribonuclease under semi-denaturing conditions. **(B)** Densitometer scans showing RNase T1 cleavage intensity in terminal loop of $(CUG)_{54}$ hairpin in the presence of different CAG25 concentrations. **(C)** Diagram showing proposed order of CAG25 binding to $(CUG)_{54}$. Note in A and B that T1 cleavage in the terminal loop is ~two-fold reduced by 200 nM CAG25, whereas 2-fold suppression of Pb cleavage in the stem requires a higher concentration of CAG25 (800-1600 nM), similar to that required for saturation of binding by gel shift assay (Fig. 1B). This supports a model in which binding at low CAG25 concentration occurs in the terminal loop and at higher concentration also along the stem.

Fig. S3

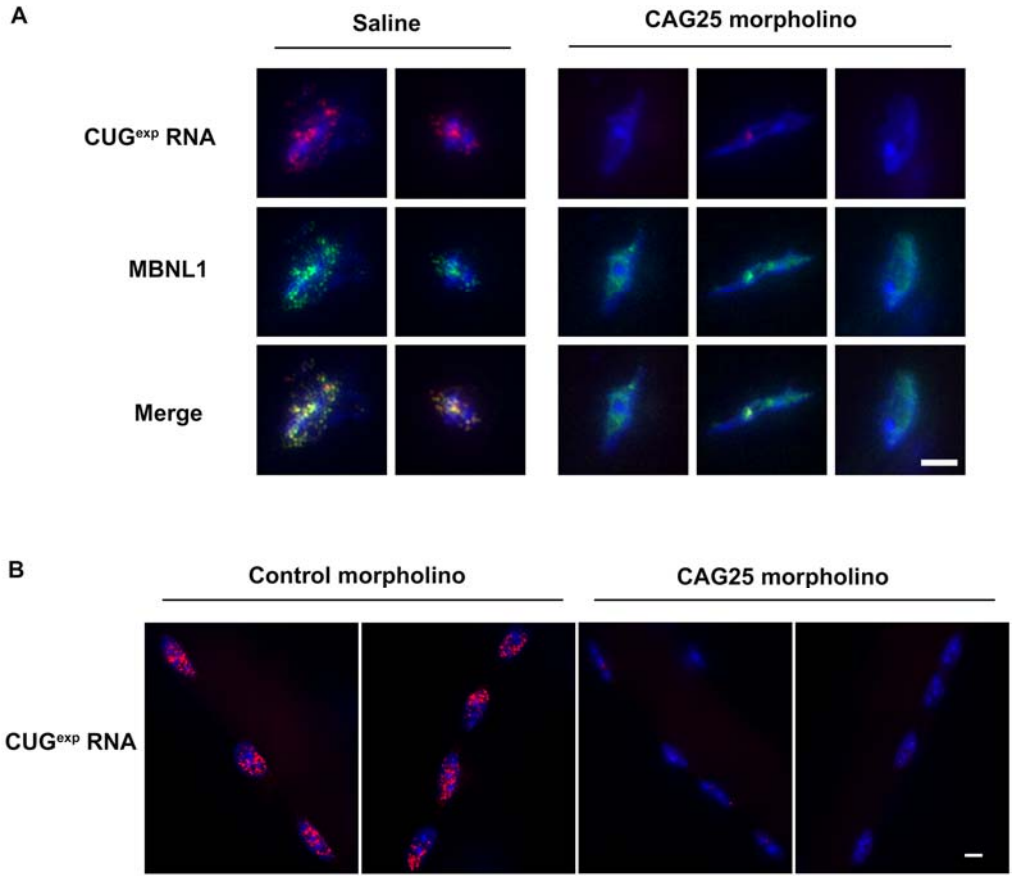

Fig. S3. Analysis of muscle sections (A) and muscle fibers (B) of *HSA*^{LR} transgenic mice shows that CAG25 morpholino disperses CUG^{exp} foci and redistributes MBNL1 protein. **(A)** Deconvolution image of FISH (red, CAG probe), immunofluorescence for MBNL1 (green), and nuclear counterstain (DAPI, blue) on transverse sections of tibialis anterior muscle. Muscle tissue was obtained 3 weeks following a single injection and electroporation of CAG25 morpholino or vehicle (saline). Scale bar = 5 μm. **(B)** Deconvolution image of FISH (red, CAG probe) and nuclear counterstain (blue) of single dissected flexor digitorum brevis muscle fibers 7 days after injection and electroporation of CAG25 or control 25mer morpholino having an unrelated sequence. Scale bar = 5 μm.

Fig. S4

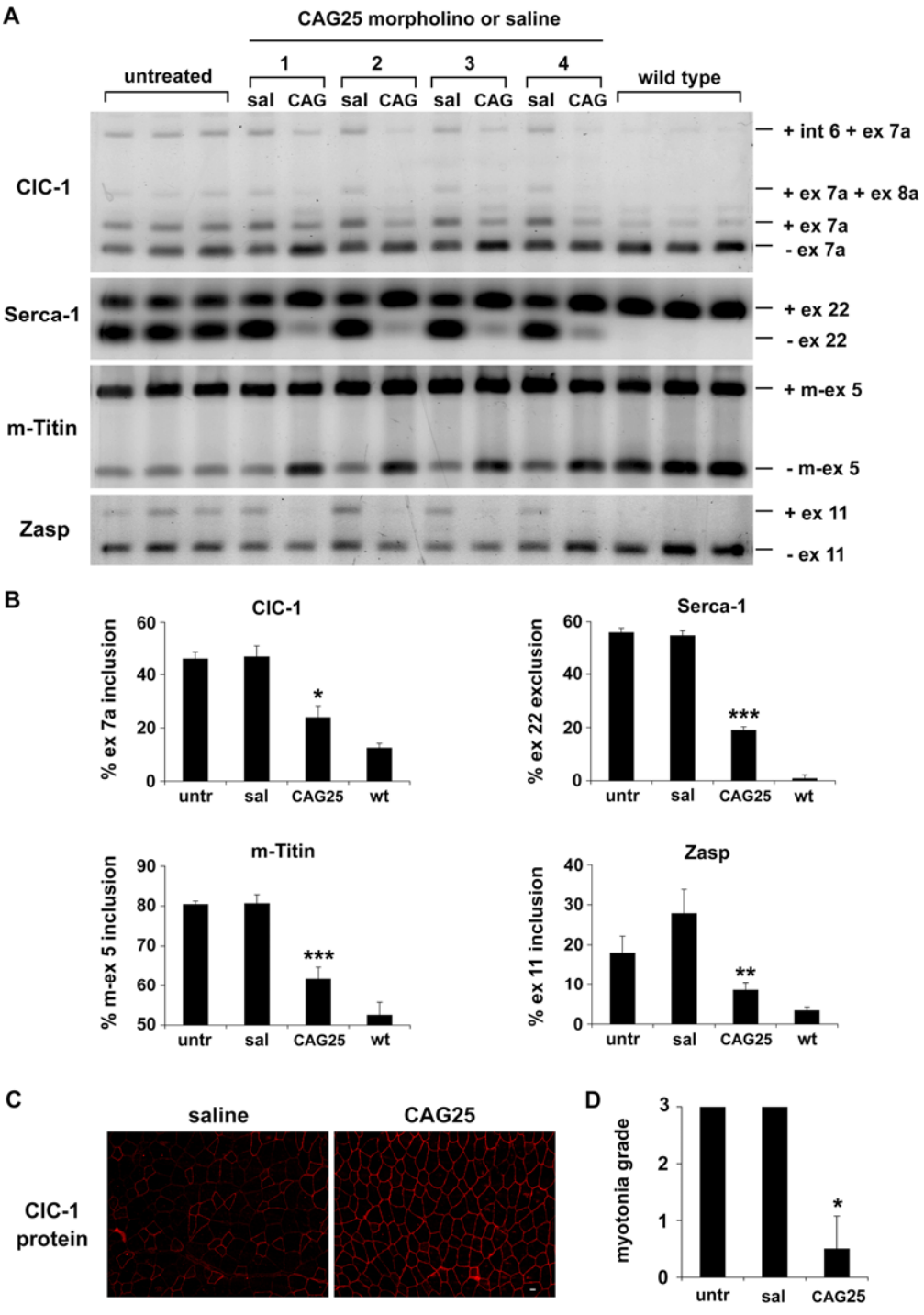
A
CAG25 morpholino or saline
untreated
1
2
3
4
wild type
sal CAG sal CAG sal CAG sal CAG
ClC-1
+ int 6 + ex 7a
+ ex 7a + ex 8a
+ ex 7a
- ex 7a
Serca-1
+ ex 22
- ex 22
m-Titin
+ m-ex 5
- m-ex 5
Zasp
+ ex 11
- ex 11
B
ClC-1
% ex 7a inclusion
Serca-1
% ex 22 exclusion
m-Titin
% m-ex 5 inclusion
Zasp
% ex 11 inclusion
untr sal CAG25 wt
C
saline
CAG25
ClC-1 protein
D
myotonia grade
untr sal CAG25

Fig. S4. Prolonged suppression of splicing defect and chloride channelopathy by a single injection of CAG25. **(A)** RT-PCR analysis of alternative splicing of ClC-1, Serca-1, m-Titin, and Zasp in *HSA*^{LR} TA muscle at 14 weeks after a single injection of CAG25 vs. vehicle alone (saline; "sal"). The ClC-1 transcripts that skip exon 7a (-ex7a) predominate in wild-type mice, and encode functional ClC-1 channels. Splice products that include exon 7a (+ex7a) encode truncated proteins, devoid of ClC-1 channel activity. All +ex7a products contain premature termination codons, and at steady state they are underrepresented due to nonsense mediated decay. **(B)** Quantitation of results shown in A, expressed as the mean ± SD percent inclusion or skipping of the indicated exon. Treatment groups n = 4 each. Untreated *HSA*^{LR} ("untr") and wild type groups n = 3 each. **P* = 0.003, ***P* = 0.0009, ****P* < 0.0001 for the CAG25 vs vehicle comparison (*t*-test). **(C)** Representative immunofluorescence for ClC-1 protein in transverse section of *HSA*^{LR} TA muscle, 14 weeks after injection with CAG25 or vehicle. Scale bar = 20 μm. **(D)** Electromyography analysis by a blinded examiner 14 weeks after injection of *HSA*^{LR} mice with CAG25 in one TA muscle and vehicle in the contralateral TA. n = 4 each; error bars denote mean ± SD **P* = 0.0001 (*t*-test).

Fig. S5

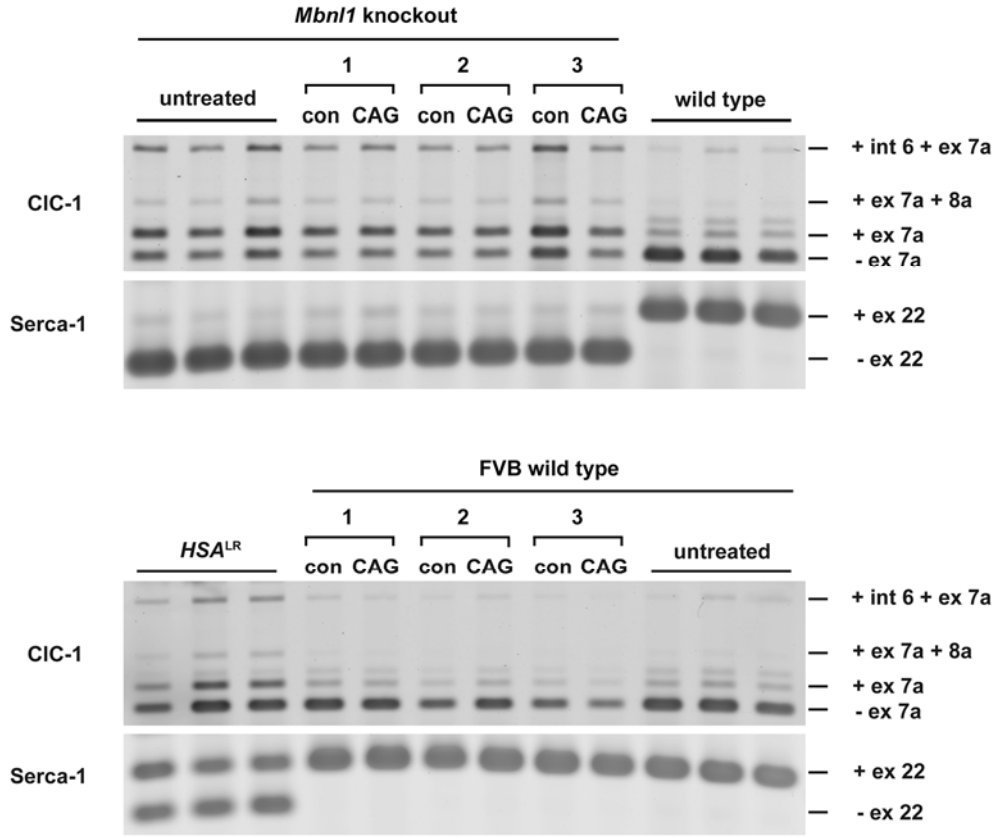

Fig S5. Alternative splicing is not affected by CAG25 in the absence of CUG^{exp} RNA. **(Upper)** *Mbnl1* knockout mice display splicing abnormalities similar to HSA^{LR} mice (*5*). RT-PCR analysis of *Mbnl1* knockout tibilais anterior muscle 3 weeks after injection of CAG25 shows no affect on splicing of ClC-1 exon 7a or Serca-1 exon 22. The contralateral ("con") tibialis anterior muscle was injected with saline. **(Lower)** Alternative splicing of ClC-1 and Serca-1 in WT mice is not affected by CAG25.

Fig. S6

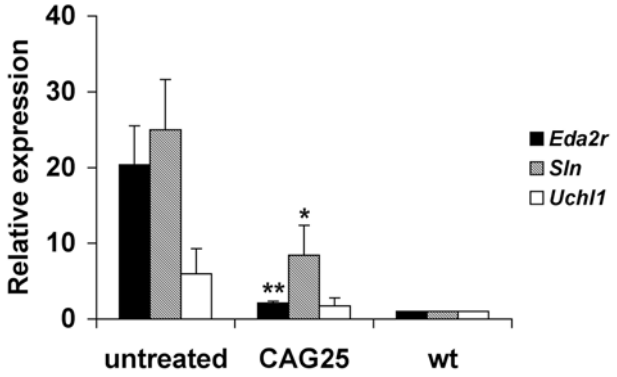

Fig. S6. CAG25 mitigates transcriptional dysregulation induced by CUG^{exp} RNA. Expression of ectodysplasin 2A receptor (*Eda2r*), sarcolipin (*Sln*), and ubiquitin carboxy-terminal hydrolase L-1 (*Uchl1*) is upregulated at the level of transcription in *Mbnl1* knockout and HSA^{LR} muscle (*10*). Shown are quantitative real-time RT-PCR analyses for these transcripts in muscle RNA. Muscle tissue was obtained 3 weeks following a single injection of CAG25, as compared to untreated HSA^{LR} or WT tibialis anterior muscles. mRNA levels were expressed in arbitrary units relative to the housekeeping gene RNA polymerase II transcription factor IIB, and then normalized to mean value = 1 for WT mice. Data are triplicate assays, $n = 3$ mice per group, expressed as mean ± SD ** $P = 0.004$; * $P = 0.020$ for CAG25 vs. untreated comparison (*t*-test).

Fig. S7

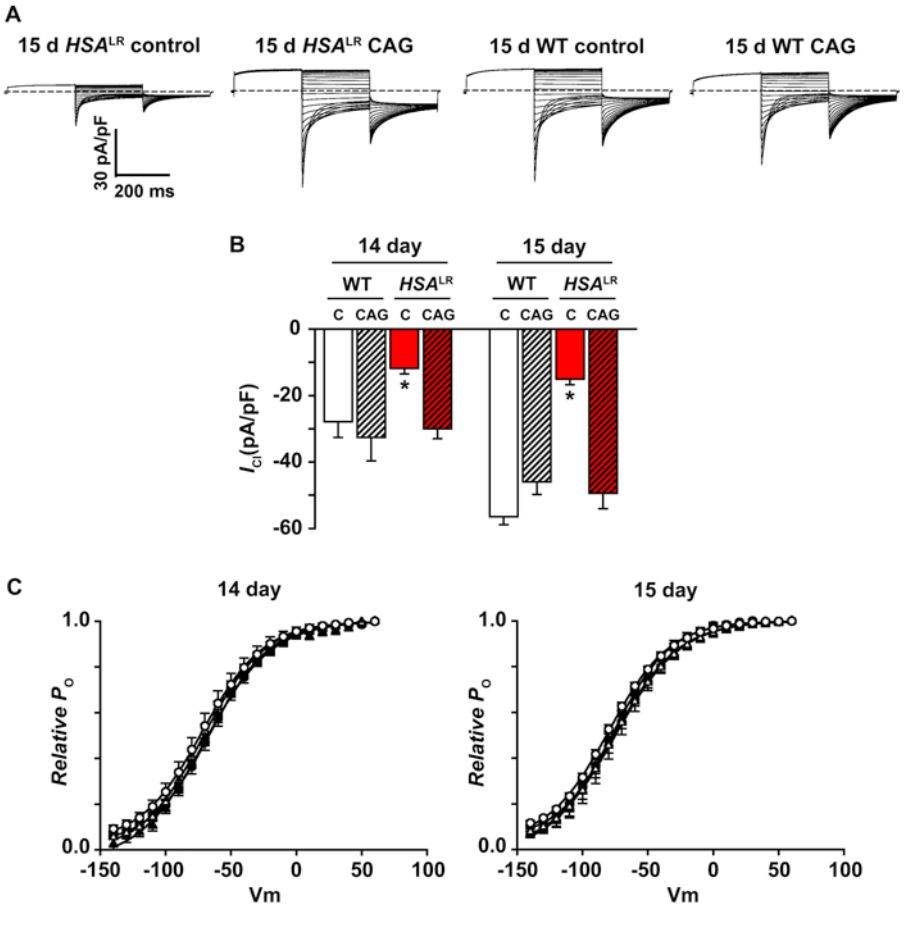

Parameters of Linear Properties and Relative Open Probabilities

		Linear Properties			Po_{rel}	
	n	C_m *pF*	R_s *kΩ*	*Tau* *μs*	*k* *mV*	$V_{1/2}$ *mV*
14 d WT control	5	338 ± 76	584 ± 12	525 ± 13	25.2 ± 0.9	-69.9 ± 2.2
14 d WT CAG	6	442 ± 38	698 ± 84	440 ± 68	23.5 ± 1.4	-71.1 ± 2.7
14 d *HSA*LR control	8	606 ± 57	933 ± 88	530 ± 34	22.7 ± 0.8	-65.7 ± 2.5
14 d *HSA*LR CAG	11	527 ± 25	795 ± 47	541 ± 90	21.7 ± 1.1	-71.0 ± 4.9
15 d WT control	5	656 ± 51	487 ± 52	452 ± 15	24.5 ± 1.7	-76.1 ± 3.5
15 d WT CAG	5	584 ± 59	659 ± 61	417 ± 42	24.8 ± 1.2	-76.0 ± 6.3
15 d *HSA*LR control	13	604 ± 43	818 ± 57	535 ± 33	20.9 ± 0.8	-74.8 ± 2.8
15 d *HSA*LR CAG	15	617 ± 34	833 ± 94	527 ± 66	23.2 ± 0.7	-80.0 ± 1.7

Fig. S7. CAG25 morpholino rescues ClC-1 channel function in skeletal muscle of *HSA*^{LR} transgenic mice. **(A)** Representative ClC-1 currents obtained from patch clamp analysis of flexor digitorum brevis (FDB) muscle fibers isolated from 15-day old *HSA*^{LR} or WT mice electroporated with CAG25 or control morpholino of unrelated sequence. The dashed lines represent 0 current levels. Currents

from control-treated *HSA*^{LR} fibers are similar to those previously reported for untreated *HSA*^{LR} fibers (*7*). **(B)** Average peak instantaneous currents at -140 mV of 14- and 15-day-old WT (white) and *HSA*^{LR} (red) mice injected and electroporated with control ("c"; open) or CAG25 (hatched) morpholino. Error bars ± SEM *$P < 0.005$ for control-treated *HSA*^{LR} fibers compared with each of the other experimental conditions; ANOVA. **(C)** Average relative channel open probability (P_O) versus voltage (Vm) curves from 14 (left) and 15 (right) day-old WT and *HSA*^{LR} mice injected and electroporated with CAG25 or control morpholino. Smooth curves through each data set were generated using a modified Boltzmann equation (*7*). **(D)** Parameters of linear properties and relative open probabilities.

Fig. S8

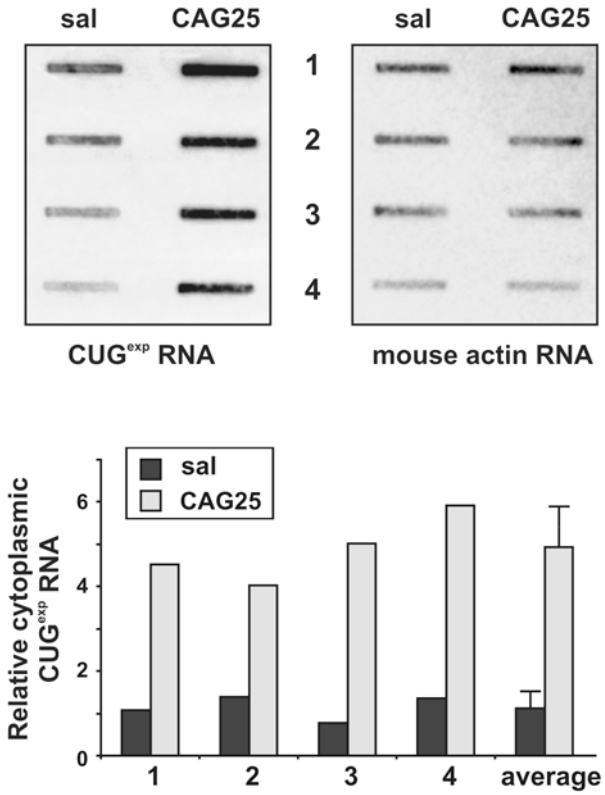

Fig. S8. CAG25 causes an increase of CUG^{exp} RNA in the cytoplasm. **(Upper)** Slot-blot hybridization of cytoplasmic RNA isolated from HSA^{LR} tibialis anterior muscle. Muscle tissue was obtained 4 weeks after a single injection of CAG25 or vehicle (saline, sal). RNA samples are the same as those analyzed in Fig. 4A. Probes were specific for human skeletal actin (*HSA*, left panel, hybridizing to sequence flanking the CUG repeat) or mouse skeletal actin (*MSA*, right panel). Specificity of *HSA* probe under these hybridization conditions is shown in Fig. S11 below. Separate blots were used for hybridization with each probe. **(Lower)** Quantification of cytoplasmic CUG^{exp} RNA relative to *MSA* is shown in the graph ($P < 0.001$; *t*-test).

Fig S9

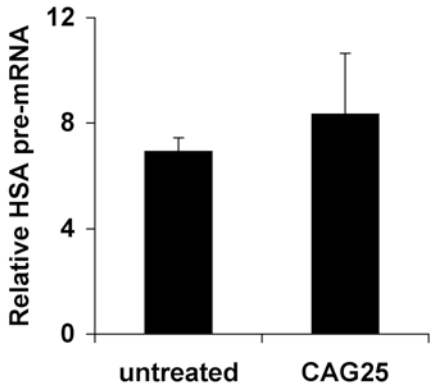

Fig. S9. Levels of *HSA* (transgene) pre-mRNA are unchanged by CAG25 morpholino. Quantitative real-time RT-PCR analysis of the human skeletal actin (transgene) pre-mRNA. Muscle RNA was treated with DNase, then amplified by qRT-PCR. PCR primers were positioned at the end of intron 1 and in exon 2, to amplify pre-spliced transgene RNA. Signal was not obtained in the absence of reverse transcriptase or in non-transgenic mice. $n = 3$ mice per group, triplicate assays per mouse, expressed as mean ± SD; $P = 0.35$ (*t*-test).

Fig. S10

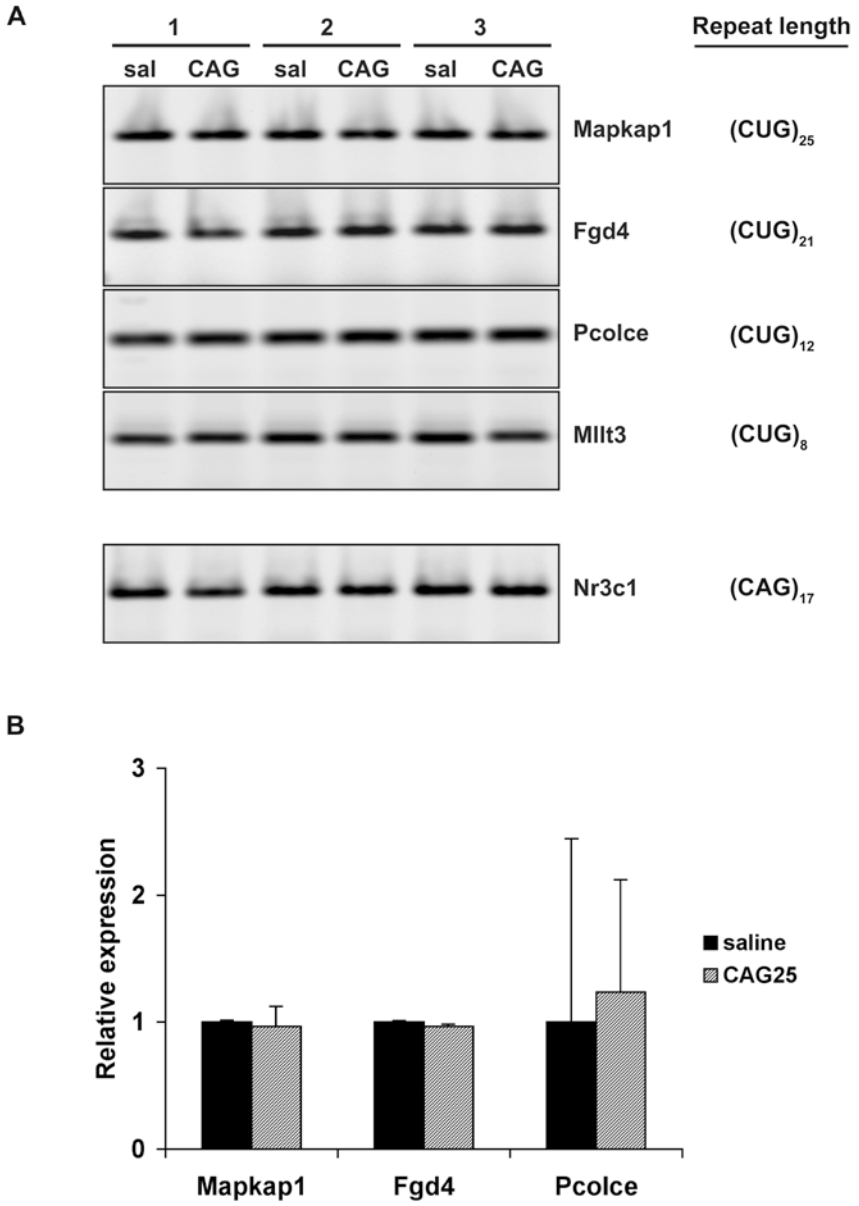

Fig. S10. CAG25 does not downregulate expression of endogenous CUG-repeat-containing transcripts in *HSA*^{LR} transgenic (**A**) or WT (**B**) mice. **(A)** Semi-quantitative RT-PCR at low cycle number (23 or 25 cycles) for expression of 4 transcripts containing untranslated CUG repeats. The number of repeats for each transcript is shown. *Nr3c1* transcript with CAG repeats serves as control. *HSA*^{LR} tibialis anterior muscle was treated with saline or CAG25 morpholino. **(B)** Quantitative real-time RT-PCR

analysis of Fgd4, Pcolce, and Mapkap1 expression in WT tibialis anterior muscle 3 weeks after injection of CAG25 vs. vehicle alone (saline, “sal”). mRNA levels are expressed in arbitrary units relative to the housekeeping gene RNA polymerase II transcription factor IIB, then normalized for mean expression = 1 in vehicle-injected muscle. n = 3 mice for each treatment, triplicate assays per sample, expressed as mean +/- S.D. $P > 0.3$ for each (t-test).

Fig. S11

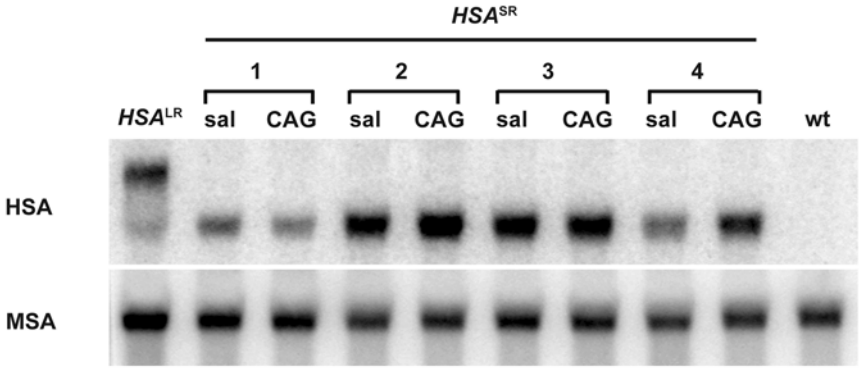

Fig. S11. CAG25 does not decrease the expression of an *HSA* transgene that contains a non-expanded repeat. Northern blot of total RNA from TA muscle isolated from *HSA*^{SR} transgenic mice that express *HSA* mRNA containing 5 CUG repeats. RNA was isolated 3 weeks after injection of CAG25. The contralateral TA muscle was injected with vehicle alone (saline, sal). Probes were specific for human skeletal actin (HSA) or mouse skeletal actin (MSA). *HSA*^{SR} transgenic mice are hemizygous, and between-mouse variability of transgene expression is greater than in *HSA*^{LR} mice (*4*).

Fig. S12

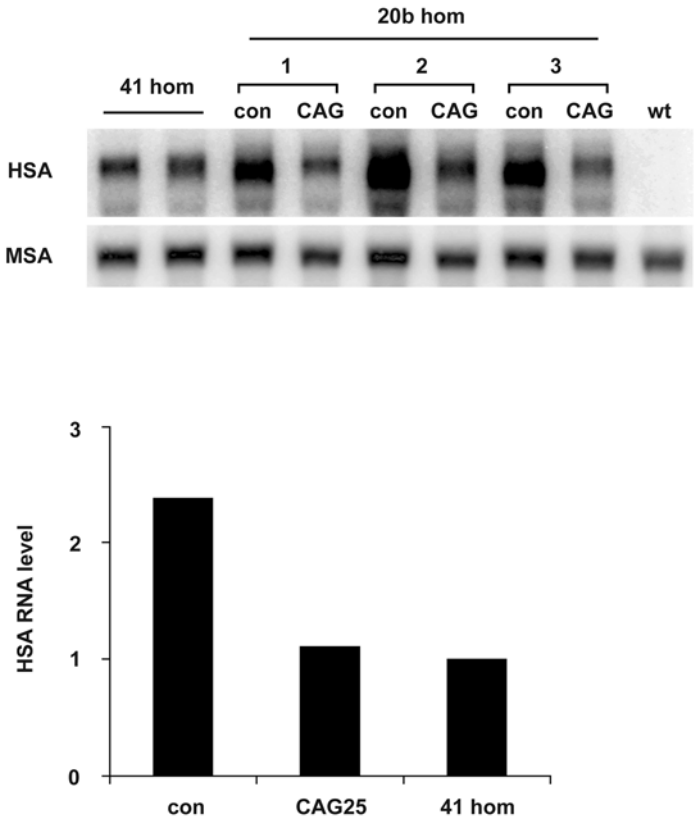

Fig. S12. Following treatment with CAG25, residual levels of CUG^{exp} RNA do not fall below the threshold level for inducing RNA disease. **(A)** Northern blot showing *HSA* RNA levels in *HSA*^{LR} mice from different founder lines. Homozygous *HSA*^{LR} mice from founder line 20b (20b hom) were used for all CAG25 experiments. Homozygous mice from founder line 41 show lower levels of transgene expression. Although the phenotype and perturbations of the transcriptome in line 41 are less severe than in line 20b (*4*, *10*), these mice nevertheless show prominent RNA foci, robust myotonia, and conspicuous changes in alternative splicing. Following treatment of line 20b mice with CAG25, residual levels of CUG^{exp} RNA are similar to line 41. Thus, reduction of CUG^{exp} RNA cannot provide a unitary explanation for therapeutic effects of CAG25 in line 20b.

Fig S13

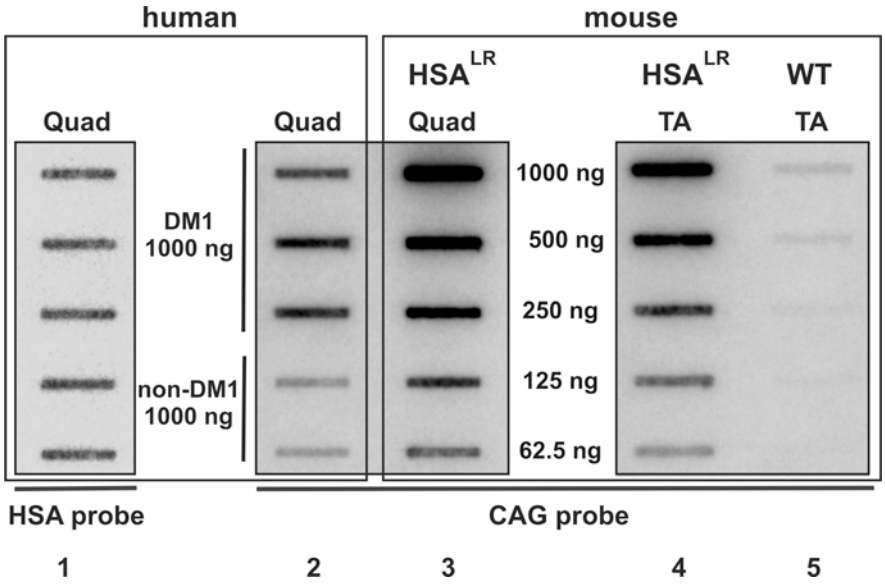

Fig. S13. Comparison of CUG^{exp} RNA amount in skeletal muscle from DM1 patients and *HSA*^{LR} mice. Slot-blot analysis of total cellular RNA (1 μg) isolated from quadriceps muscle from DM1 patients or individuals without muscle disease ("non-DM1"), as compared to the indicated amount of total cellular RNA from quadriceps ("Quad") or tibialis anterior ("TA") muscle of *HSA*^{LR} or wild-type mice. Hybridizations were performed with radiolabeled CAG repeat DNA probe (lanes 2 through 5) or human skeletal actin (HSA) probe (lane 1, loading control). When normalized for background hybridization of CAG probe in non-disease controls, the hybridization signal from DM1 RNA is 4-8 times lower than the same quantity of RNA isolated from *HSA*^{LR} quadriceps, and 2-4 times lower than *HSA*^{LR} tibialis anterior.

Fig. S14

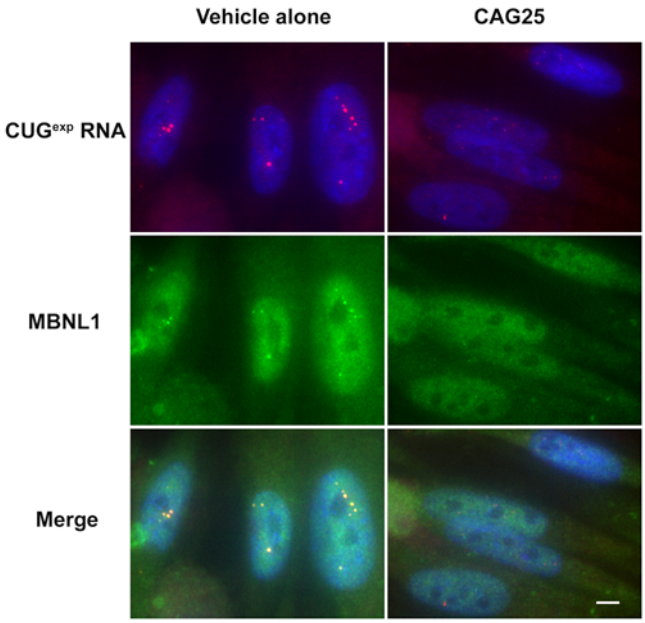

Fig. S14. CAG25 morpholino reduces RNA and MBNL1 foci in human DM1 fibroblasts. Representative fluorescence *in situ* hybridization for CUG^{exp} RNA combined with immunofluorescence analysis for MBNL1 protein expression in human DM1 fibroblasts (2000 CTG repeats) treated with CAG25 morpholino or vehicle alone for 48 hours. Because DMPK expression in fibroblasts is low, the level of CUG^{exp} accumulation is not sufficient to sequester MBNL1. Scale bar = 5 μm.

Table S1. Primers used for RT-PCR amplification of endogenous transcripts containing either CUG or CAG repeats (control).

Primer name	Sequence (5′-3′)	Repeat length and its location	No. of PCR cycle (Ta)
Mapkap1 F Mapkap1 R	ACCCTGTTACGAATCAGAAAGCCA TCTGGAAGCTGAAGCTTGTTCG	$(CUG)_{25}$, 3′ UTR	25 (55^{o}C)
Fgd4 F Fgd4 R1	ACTAGCAGCTCGGAACACATCAGC TTCAGGAAGCTTTGGCAAGACTGG	$(CUG)_{21}$, 3′ UTR	25 (55^{o}C)
Pcolce F Pcolce R	TGGGGCCATTCCTTTTGGCCTG AGACCTCCAGAGCATCGTAGC	$(CUG)_{12}$, 5′ UTR	23 (55^{o}C)
Mllt3 F Mllt3 R	TCTCATGTCAAGATGGGAAAGGTC CCGAGTCATTGTCATTGTCCTCTG	$(CUG)_{8}$, 5′ UTR	23 (55^{o}C)
Nr3c1 F Nr3c1 R	TTGGGGGCTATGAACTTCGCAGG TCGAGCTTCCAGGTTCATTCCAGC	$(CAG)_{17}$, ORF	23 (55^{o}C)

Supporting References

1. Y. Yuan *et al.*, *Nucleic Acids Res* **35**, 5474 (2007).
2. M. B. Warf, J. A. Berglund, *RNA* **13**, 2238 (2007).
3. J. W. Miller *et al.*, *Embo J* **19**, 4439 (2000).
4. A. Mankodi *et al.*, *Science* **289**, 1769 (2000).
5. R. N. Kanadia *et al.*, *Science* **302**, 1978 (2003).
6. T. M. Wheeler, J. D. Lueck, M. S. Swanson, R. T. Dirksen, C. A. Thornton, *J Clin Invest* **117**, 3952 (2007).
7. J. D. Lueck, A. Mankodi, M. S. Swanson, C. A. Thornton, R. T. Dirksen, *J Gen Physiol* **129**, 79 (2007).
8. X. Lin *et al.*, *Hum Mol Genet* **15**, 2087 (2006).
9. C. Bertoni *et al.*, *Proc Natl Acad Sci U S A* **103**, 419 (2006).
10. R. J. Osborne *et al.*, *Hum Mol Genet* **18**, 1471 (2009).